Nuclear Instruments and Methods in Physics Research A 645 (2011) 321–326

Contents lists available at ScienceDirect

Nuclear Instruments and Methods in Physics Research A

journal homepage: www.elsevier.com/locate/nima

Upgraded G-optk program for electron gun characterization

K. Nagasao [a,*], M. Takebe [a], W. Ushio [a], S. Fujita [a,b], T. Ohye [b], H. Shimoyama [b]

[a] SHIMADZU Corporation, 1, Nishinokyo-Kuwabaracho, Nakagyo-ku, Kyoto 604-8511, Japan
[b] Meijo University, 1-501, Shiogamaguchi, Tempaku-ku, Nagoya 468-8502, Japan

ARTICLE INFO

Available online 22 December 2010

Keywords:
Source property
Optical parameter
Ray tracing
Paraxial trajectory theory
Aberration

ABSTRACT

The generalized trajectory theory (the G-optk program) has been extended in order to make the method applicable to electron guns with curved and/or asymmetric cathodes. The object-image analysis mode has also been added. Enhanced capability of the upgraded G-optk program was demonstrated by applying the program to three electron optical systems: (a) the point cathode gun, (b) the hairpin-type cathode gun, and (c) the LEEM objective lens. The Canonical Mapping Transformation (CMT) diagrams were calculated both by direct ray tracing and by the upgraded G-optk program. In each case, it was found that the upgraded program reproduces well the results obtained by ray tracing. The generalized trajectory method has several advantages over direct ray tracing, such as substantially lighter calculation load and easy interpretation of the calculation results in terms of the optical parameters.

1. Introduction

The characterization of cathode rays inside electron guns is in principle possible by use of the trajectory theory (the paraxial trajectory and aberration theory), as opposed to conventional direct ray tracing. The key to the successful treatment of cathode rays with large inclination angles lies in an accurate reproduction of parabolic-shape ray paths in accelerating field in front the cathode. Several schemes were proposed to represent parabolic rays within the paraxial trajectory scheme [1,2].

The present authors have found that a simple mathematical relation exists between the ray condition (position and slope) on the cathode surface and that at the crossover plane (see Fig. 1) [3]. If a 2D–2D mapping, $(\xi_x, u_x = \sin\alpha) \geq (\eta_{cx}, v_x = \sin\beta)$, is considered, it must satisfy the canonical condition and can be characterized by a set of transformation parameters. We shall designate the mapping as the CMT diagram. A scrutinized review of the conventional trajectory theory has revealed that mapping can be approximated by third-order polynomials [4]:

$$\eta_{cx}(\xi_x, u_x) = f\sqrt{\Phi_0/\Phi_1}\,u_x + \sum_{k+l=3} a_{kl}\xi_x^k u_x^l \tag{1a}$$

$$v_x(\xi_x, u_x) = -\xi_x/f + m u_x + \sum_{k+l=3} b_{kl}\xi_x^k u_x^l \tag{1b}$$

where f, m, a_{kl} and b_{kl} are optical parameters defined by these equations that stand for electron gun focal length, modified angular magnification and aberration coefficients, respectively. For the evaluation of the polynomial coefficients, a method very similar to that used in the conventional trajectory theory can be used. The mathematical expression for the mapping is given by

$$\begin{pmatrix} \eta_{cx} \\ v_x \end{pmatrix} = \begin{pmatrix} g(z_c) & h(z_c) \\ g'(z_c) & h'(z_c) \end{pmatrix} \left\{ \begin{pmatrix} \xi_x \\ u_x \end{pmatrix} + \frac{1}{\sqrt{2me\Phi_0}} \begin{pmatrix} -\frac{\partial V^I}{\partial u_x} \\ \frac{\partial V^I}{\partial \xi_x} \end{pmatrix} \right\}, \tag{2}$$

where $V^I(\xi_x, u_x)$ represents the aberration integral arising from the fourth-order Lagrangian terms in the action integral, of which the formula is given by Eq. (13) in Ref. [4]. The principal paraxial trajectories are represented by $g(z)$ and $h(z)$.

An apparently trivial calculus difference from the conventional theory consists of replacing the trigonometric function tan with sin in the trajectory slope definition. The physical significance behind the choice of sin is that in assigning the paraxial trajectory to the cathode ray, the transverse momentum of the ray is considered more important, rather than its slope. Fig. 2 shows how the paraxial trajectories are assigned to a parabolic cathode ray in each case. In the proposed method a trajectory that has the same transverse momentum as the cathode ray is adopted in the paraxial approximation.

We reported in the previous conference (CPO-7, Cambridge UK) the implementation of the generalized trajectory theory in the G-optk program for electron gun characterization [5]. The new approach can offer a suite of optical parameters (the coefficients), including aberration coefficients, to define the electron gun characteristics. However, the applicability of the program has so far been limited to electron guns that have flat cathodes; the trajectory theory can perform calculation only from one reference plane to the other plane. It is desirable to lift the limitation and enable the G-optk program to deal with a wider range of electron guns.

* Corresponding author.
E-mail address: nagasao@shimadzu.co.jp (K. Nagasao).

0168-9002/$ - see front matter © 2010 Elsevier B.V. All rights reserved.
doi:10.1016/j.nima.2010.12.140

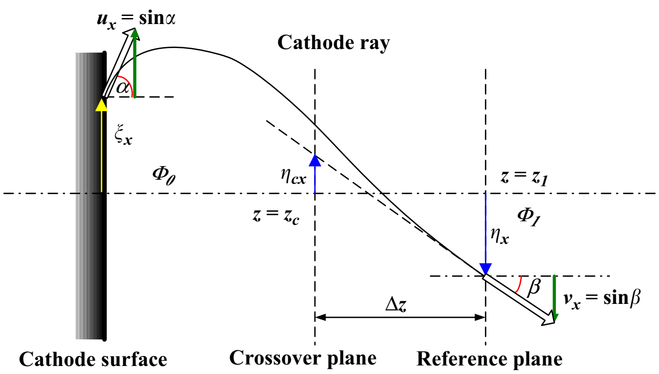

Fig. 1. Trajectory variables used in the CMT diagram.

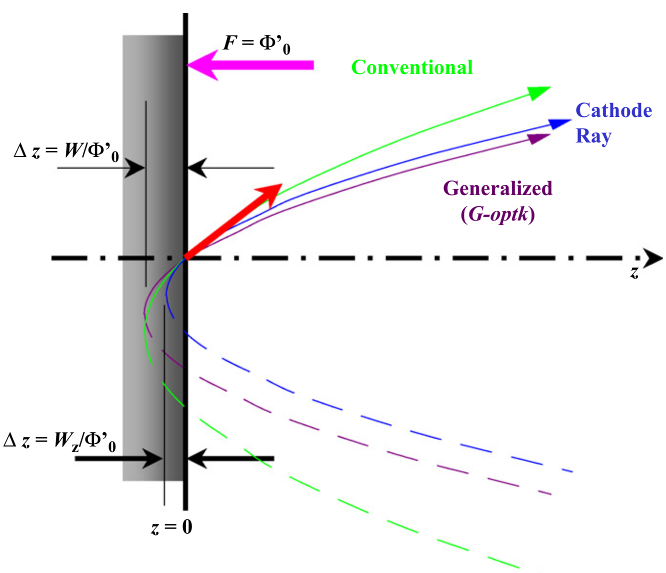

Fig. 2. Assignments of paraxial trajectories in the conventional and generalized trajectory theories.

In the present paper we shall report the upgrade of the G-optk program, by which the characterization of wider range electron guns with curved cathodes, such as pointed emitters and hairpin-type cathodes, has become possible. In addition, the program now has the object-image analysis mode as well as the crossover analysis. An application to the LEEM objective lens will be presented.

2. Mathematical formulations

In this section a mathematical formulation is first presented to extend the applicability of the generalized trajectory theory to deal with curved cathodes like cold field emitters. As indicated in Fig. 3, a connecting space is introduced between the cathode surface and the first reference plane. The actual ray condition on the cathode is transformed into the trajectory condition at the reference plane placed tangent to the curved cathode tip, and the actual trajectory calculation is commenced from the reference plane. In accordance with the cathode tip radius ρ, we need to modify the definition of the principal paraxial trajectories $g(z)$ and $h(z)$ as

$$g(z_0) = 1, \quad g'(z_0) = 1/\rho \tag{3a}$$

$$h(z_0) = 1, \quad h'(z_0) = 1 \tag{3b}$$

where z_0 is the initial coordinate in paraxial trajectory calculation.

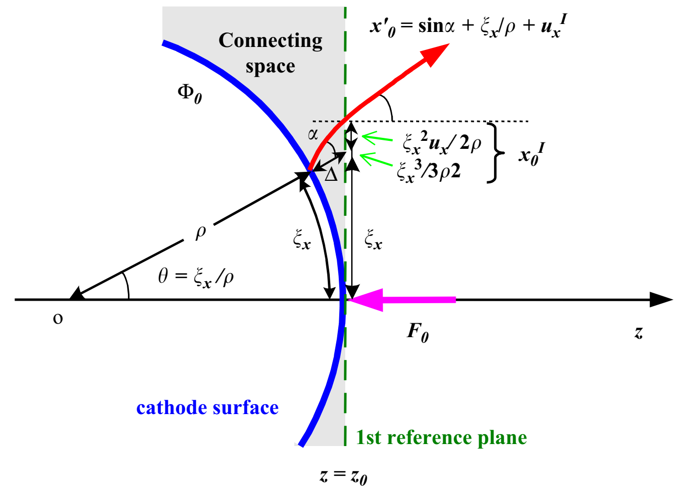

Fig. 3. Transformation of the trajectory conditions in the connecting space.

The principal trajectory $g(z)$ now has a nonzero initial gradient, $g'(z_0) = \rho^{-1}$, to properly represent rays emanating in surface normal direction.

The electron acceleration due to the cathode surface field in the connecting space, which results in an increase in the transverse momentum p_x at the reference plane, has been found to significantly influence the estimate of the spherical aberration coefficient. In order to reflect the effects it is necessary to modify the transformation Eq. (2) as follows:

$$\begin{pmatrix}\eta_{cx}\\ v_x\end{pmatrix} = \begin{pmatrix} g(z_c) & h(z_c)\\ g'(z_c) & h'(z_c)\end{pmatrix}\left\{\begin{pmatrix}\xi_x + x_0^I\\ u_x+[u_x^I - x_0^I/\rho]\end{pmatrix} + \frac{1}{\sqrt{2me\Phi_0}}\begin{pmatrix} -\frac{\partial V^I}{\partial u_x}\\ \frac{\partial V^I}{\partial \xi_x}\end{pmatrix}\right\}, \tag{4}$$

in which the trajectory initial condition is corrected by x_0^I and u_x^I. Please refer to the literature [6] for details.

A further modification has also been made in order to deal with an asymmetric field encountered, for example, in analyzing the hairpin-type cathode gun. In this case the transformations in the x–z plane and in the y–z plane are different because of the lack of axial symmetry in the gun geometry and the revised transformation is given by

$$\begin{pmatrix}\eta_c\\ v\end{pmatrix} = \begin{pmatrix} g(z_c) & h(z_c)\\ g'(z_c) & h'(z_c)\end{pmatrix}\left\{\begin{pmatrix}\xi + r_0^I\\ u+[u^I - r_0^I/\rho/] + \Delta(1/R)\bar{\xi}\end{pmatrix} + \frac{1}{\sqrt{2me\Phi_0}}\begin{pmatrix} -2\frac{\partial V^I}{\partial \bar{u}}\\ 2\frac{\partial V^I}{\partial \bar{\xi}}\end{pmatrix} + \frac{1}{\sqrt{2me\Phi_0}}\begin{pmatrix} -2\frac{\partial V^A}{\partial \bar{u}}\\ 2\frac{\partial V^A}{\partial \bar{\xi}}\end{pmatrix}\right\} \tag{5}$$

Note that the complex number convention for representing simultaneously both the x and y components is adopted in the above formula. The upper bar represents taking complex conjugate of each variable. Please refer to a separate literature for a detailed explanation [7].

Two new terms are added to Eq. (4). The last term containing the aberration integral V^A originates from the quadrupole field present. The Laplace potential is expanded into components on the basis of their dependence on the azimuth angle φ:

$$\begin{aligned}\varphi(\mathbf{r}) = {} & \Phi(z) - \frac{r^2}{4}\Phi''(z) + \frac{r^4}{64}\Phi^{(4)}(z) + \cdots \\ & + \left\{\frac{1}{2}q_1(z) - \frac{1}{24}q_1''(z)r^2 + \cdots\right\} r^2\cos 2\varphi \\ & + \left\{\frac{1}{24}o_1(z) + \cdots\right\} r^4\cos 4\varphi \end{aligned} \tag{6}$$